J|A|C|S
ARTICLES
Published on Web 03/23/2004

ansa-Zirconocene Ester Enolates: Synthesis, Structure, Reaction with Organo-Lewis Acids, and Application to Polymerization of Methacrylates

Andrew D. Bolig and Eugene Y.-X. Chen*

Contribution from the Department of Chemistry, Colorado State University, Fort Collins, Colorado 80523-1872

Received December 5, 2003; E-mail: eychen@lamar.colostate.edu

Abstract: The synthesis, structural characterization, and abstraction chemistry of *ansa*-zirconocene ester enolate complexes relevant to the isospecific polymerization of methacrylates are reported. Reactions of *rac*-(EBI)ZrMe(OTf) and *rac*-(EBI)Zr(OTf)$_2$ [EBI = $C_2H_4(Ind)_2$] with 1 and 2 equiv of lithium isopropylisobutyrate in toluene produce the first examples of *ansa*-zirconocene mono- and diester enolate complexes: *rac*-(EBI)ZrMe[OC(O^{i}Pr)=CMe$_2$] (**1**) and *rac*-(EBI)Zr[OC(O^{i}Pr)=CMe$_2$]$_2$ (**2**) in 89% and 50% isolated yields, respectively. The reaction of **1** with B(C$_6$F$_5$)$_3$ was investigated in six different organic solvents; in THF at ambient temperature, this reaction cleanly produces the isolable cationic *ansa*-zirconocene ester enolate complex *rac*-(EBI)Zr$^+$(THF)[OC(O^{i}Pr)=CMe$_2$][MeB(C$_6$F$_5$)$_3$]$^-$ (**3**) in quantitative yield. The analogous reaction of **1** with Al(C$_6$F$_5$)$_3$ in toluene, however, proceeds through a proposed novel, intramolecular proton transfer process in which propylene is eliminated from the isopropoxy group, subsequently producing a carboxylate-bridged tight ion pair *rac*-(EBI)Zr$^+$(Me)OC(^{i}Pr)OAl(C$_6$F$_5$)$_3^-$ (**4**). In addition to standard spectroscopic and analytical characterizations for the isolated complexes **1**−**4**, complexes **2** and **4** have also been structurally characterized by X-ray diffraction studies. Polymerization of methyl methacrylate (MMA) and *n*-butyl methacrylate (BMA) has been investigated using complexes **1**, **3**, and **4**. Both the isolated cationic **3** and neutral **1** (the latter combined with B(C$_6$F$_5$)$_3$ in situ) are highly active (10 min for quantitative MMA conversion) and highly isospecific ([*mm*] > 95% for PMMA; [*mm*] > 99% for PBMA) via enantiomorphic-site control, producing polymethacrylates with extremely narrow molecular weight distributions (M_w/M_n = 1.03). The aluminate complex **4**, however, produces syndiotactic PMMA predominantly via chain-end control.

Introduction

Collins and co-workers showed that a two-component system consisting of neutral zirconocene ester enolate complex Cp$_2$ZrMe[OC(O*t*Bu)=CMe$_2$] as initiator and cationic zirconocene complex [Cp$_2$ZrMe(THF)]$^+$[BPh$_4$]$^-$ as catalyst polymerizes methyl methacrylate (MMA) in a living fashion to high molecular weight, syndiotactic-rich poly(methyl methacrylate) (PMMA).[1] The ability to isolate the nonbridged, bis(Cp) zirconocene ester enolate in its pure state provided a critical mechanistic tool that enabled detailed kinetic studies, thereby revealing a group-transfer-type[2] bimetallic propagating polymerization mechanism for MMA polymerization mediated by the two-component system comprising either simple bis(Cp) zirconocene dimethyl or zirconocene methyl enolate in combination with a zirconocenium activator.[1,3]

Since the initial reports of MMA polymerization by *achiral* zirconocenes such as neutral chloro-zirconocene enolate Cp$_2$ZrCl[OC(OMe)=CMe$_2$][4] and cationic zirconocene complex [Cp$_2$ZrMe(THF)]$^+$[BPh$_4$]$^-$ in combination with neutral Cp$_2$ZrMe$_2$,[5] several reports have appeared that investigated *chiral* cationic *ansa*-zirconocene complexes to produce highly isotactic PMMA via an enantiomorphic, site-control mechanism.[1b,6] Although the cationic *ansa*-zirconocene ester enolates (**A**) have been suggested as the active propagating species that adopt a monometallic, 1,4-conjugated addition pathway (**A**→**B**) similar to Yasuda's neutral lanthanocene-mediated MMA polymerization process,[7] there are no polymerization studies using the isolated chiral *ansa*-zirconocene ester enolates, either in their neutral or cationic form. Therefore, the mechanism of the MMA

(1) (a) Li, Y.; Ward, D. G.; Reddy, S. S.; Collins, S. *Macromolecules* **1997**, *30*, 1875−1883. (b) Collins, S.; Ward, D. G.; Suddaby, K. H. *Macromolecules* **1994**, *27*, 7222−7224.
(2) (a) Sogah, D. Y.; Hertler, W. R.; Webster, O. W.; Cohen, G. M. *Macromolecules* **1987**, *20*, 1473−1488. (b) Webster, O. W.; Hertler, W. R.; Sogah, D. Y.; Farnham, W. B.; RajanBabu, T. V. *J. Am. Chem. Soc.* **1983**, *105*, 5706−5708.
(3) Bandermann, F.; Ferenz, M.; Sustmann, R.; Sicking, W. *Macromol. Symp.* **2001**, *174*, 247−253.
(4) Farnham, W. B.; Hertler, W. U.S. Pat. 4,728, 706, 1988.
(5) Collins, S.; Ward, S. G. *J. Am. Chem. Soc.* **1992**, *114*, 5460−5462.
(6) (a) Karanikolopoulos, G.; Batis, C.; Pitsikalis, M.; Hadjichristidis, N. *Macromol. Chem. Phys.* **2003**, *204*, 831−840. (b) Bolig, A. D.; Chen, E. Y.-X. *J. Am. Chem. Soc.* **2002**, *124*, 5612−5613. (c) Frauenrath, H.; Keul, H.; Höcker, H. *Macromolecules* **2001**, *34*, 14−19. (d) Bolig, A. D.; Chen, E. Y.-X. *J. Am. Chem. Soc.* **2001**, *123*, 7943−7944. (e) Cameron, P. A.; Gibson, V.; Graham, A. J. *Macromolecules* **2000**, *33*, 4329−4335. (f) Chen, Y.-X.; Metz, M. V.; Li, L.; Stern, C. L.; Marks, T. J. *J. Am. Chem. Soc.* **1998**, *120*, 6287−6305. (g) Deng, H.; Shiono, T.; Soga, K. *Macromolecules* **1995**, *28*, 3067−3073.
(7) (a) Yasuda, H.; Yamamoto, H.; Yamashita, M.; Yokota, K.; Nakamura, A.; Miyake, S.; Kai, Y.; Kanehisa, N. *Macromolecules* **1993**, *26*, 7134−7143. (b) Yasuda, H.; Yamamoto, H.; Yokota, K.; Miyake, S.; Nakamura, A. *J. Am. Chem. Soc.* **1992**, *114*, 4908−4909.

polymerization mediated by chiral *ansa*-zirconocene complexes still remains unconfirmed.

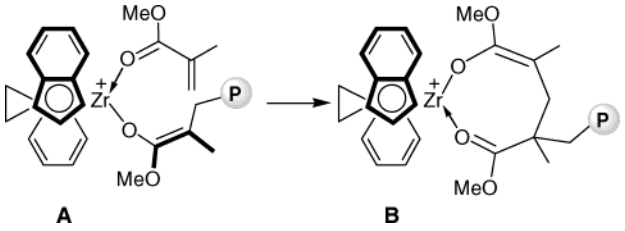

Efforts to answer this fundamental question have been challenged by the synthetic difficulty in the preparation of chiral *ansa*-zirconocene ester enolates.[8] While the group four metallocene aldehyde or ketone enolates are accessible via a variety of synthetic approaches,[9] the synthesis of simple nonbridged zirconocene ester enolates is limited to the reaction of zirconocene mono- or dichlorides with lithium alkylisobutyrates.[1] This approach is also successful for the synthesis of a prochiral, constrained-geometry zirconium bis(enolate) complex, but unsuccessful for the synthesis of chiral *ansa*-zirconocene ester enolates.[8] We previously reported that zirconocene ester enolates can also be generated by in situ reaction of zirconocene imido complexes with MMA, but producing cyclic zirconocene enolates.[10] Structural characterization of zirconocene ester enolates is another challenging aspect of this chemistry. In sharp contrast to the crystalline titanium ester enolate complex Cp_2-Ti(Cl)[OC(OMe)═CMe_2], which has been structurally characterized by X-ray diffraction,[11] simple bis(Cp) zirconocene ester enolate complexes are typically not crystalline and exist as viscous oils. The first reported structurally characterized bis-(Cp) zirconocene ester enolate is not the expected species, but an unexpected zirconocene *β-keto ester* enolate, which was formed presumably via a Claisen type condensation or a ketene intermediate; this viscous red-orange oily product finally crystallized after 6 months.[12]

Metallocene bis(triflate) complexes have been employed in homogeneous catalysis, including aldol condensations[13] and Diels−Alder reactions.[14] Collins and co-workers reported the preparation of *ansa*-metallocene bis(triflate) complexes such as *rac*-(EBTHI)Zr(OTf)$_2$ [EBTHI = ethylene bis(tetrahydroindenyl)] via the reaction of the *ansa*-metallocene dimethyl precursor and 2 equiv of triflic acid at low temperatures.[14b] Buchwald and co-workers briefly mentioned in situ generation of the mono-triflate complex (EBTHI)ZrMe(OTf) by treating the corresponding dimethyl precursor with 1 equiv of triflic acid at −78 °C.[15] For simple bis(Cp) metallocenes, Luinstra showed that mono-triflate complexes Cp_2MMe(OTf) (M = Zr, Ti) can be conveniently prepared from the comproportionation reaction involving Cp_2MMe_2 and $Cp_2M(OTf)_2$.[16]

The central objective of the present study was to isolate and characterize the elusive chiral *ansa*-zirconocene ester enolates as well as to investigate the reactions of these isolated ester enolates with strong organo-Lewis acids M(C_6F_5)$_3$ (M = B, Al), reactions of which are directly relevant to the isospecific MMA polymerization mediated by chiral *ansa*-zirconocene complexes. Furthermore, we hoped to produce crystalline zirconocene ester enolates so that they could be structurally characterized. To achieve these goals, we explored the possibility of using *ansa*-zirconocene triflate precursors for the synthesis, after our many unsuccessful attempts with *ansa*-zirconocene chloride precursors. We report here the first isolation of *ansa*-zirconocene ester enolate complexes (both mono- and diester enolates) as well as the structural characterization of the diester enolate complex by X-ray diffraction studies. Reactions of the *ansa*-zirconocene methyl monoester enolate with strong organo-Lewis acids M(C_6F_5)$_3$ produce the corresponding cationic *ansa*-zirconocene ester enolate complex (M = B) and, very interestingly, a cationic *ansa*-zirconocene methyl complex (M = Al). These cationic complexes have been isolated and characterized spectroscopically and analytically, and the solid-state structure of the cationic species derived from the reaction with the alane has also been characterized by X-ray diffraction. Both the isolated cationic and neutral ester enolates (the latter combined with B(C_6F_5)$_3$ in situ) are highly active and isospecific for polymerization of methacrylates, producing polymethacrylates with extremely narrow molecular weight distributions and high initiator efficiency.

Experimental Section

Materials and Methods. All syntheses and manipulations of air- and moisture-sensitive materials were carried out in flamed Schlenk-type glassware on a dual-manifold Schlenk line, a high vacuum line (10^{-5} to 10^{-7} Torr), or in an argon-filled glovebox (<1.0 ppm oxygen and moisture). NMR-scale reactions (typically in a 0.02 mmol scale) were conducted in Teflon-valve-sealed J. Young-type NMR tubes. HPLC grade organic solvents were first saturated with nitrogen during filling the solvent reservoir and then dried by passage through activated alumina (for diethyl ether, THF, and methylene chloride) followed by passage through Q-5 supported copper catalyst (for toluene and hexanes) stainless steel columns. Benzene-d_6, toluene-d_8, and THF-d_8 were dried over sodium/potassium alloy and vacuum-distilled or filtered, whereas C_6D_5Br, $CDCl_3$, and *o*-dichlorobenzene were dried over activated Davison 4 Å molecular sieves. NMR spectra were recorded on either a Varian Inova 300 (FT 300 MHz, ^{1}H; 75 MHz, ^{13}C; 282 MHz, ^{19}F) or a Varian Inova 400 spectrometer. Chemical shifts for ^{1}H and ^{13}C spectra were referenced to internal solvent resonances and are reported as parts per million relative to tetramethylsilane, whereas ^{19}F NMR spectra were referenced to external $CFCl_3$. Elemental analyses were performed by Desert Analytics, Tucson, Arizona.

(8) Nguyen, H.; Jarvis, A. P.; Lesley, M. J. G.; Kelly, W. M.; Reddy, S. S.; Taylor, N. J.; Collins, S. *Macromolecules* **2000**, *33*, 1508−1510.
(9) For representative examples of group four metallocene aldehyde and ketone enolates, see (a) Spaether, W.; Klaβ, K.; Erker, G.; Zippel, F.; Fröhlich, R. *Chem. Eur. J.* **1998**, *4*, 1411−1417. (b) Veya, P.; Floriani, C.; Chiesi-Villa, A.; Rizzoli, C. *Organometallics* **1993**, *12*, 4892−4898. (c) Bertz, S. H.; Dabbagh, G.; Gibson, C. P. *Organometallics* **1988**, *7*, 563−565. (d) Gibson, C. P.; Dabbagh, G.; Bertz, S. H. *J. Chem. Soc., Chem. Commun.* **1988**, 603−605. (e) Curtis, M. D.; Thanedar, S.; Butler, W. M. *Organometallics* **1984**, *3*, 1855−1859. (f) Stille, J. R.; Grubbs, R. H. *J. Am. Chem. Soc.* **1983**, *105*, 1664−1665.
(10) Jin, J.; Mariott, W. R.; Chen, E. Y.-X. *J. Polym. Sci., Part A: Polym. Chem.* **2003**, *41*, 3132−3142.
(11) Hortmann, K.; Diebold, J.; Brintzinger, H.-H. *J. Organomet. Chem.* **1993**, *445*, 107−109.
(12) Stuhldreier, T.; Keul, H.; Höcker, H.; Englert, U. *Organometallics* **2000**, *19*, 5231−5234.
(13) (a) Lin, S.; Bondar, G. V.; Levy, C. J.; Collins, S. *J. Org. Chem.* **1998**, *63*, 1885−1892. (b) Hollis, T. K.; Bosnich, B. *J. Am. Chem. Soc.* **1995**, *117*, 4570−4581.
(14) (a) Bondar, G. V.; Aldea, R.; Levy, C. J.; Jaquith, J. B.; Collins, S. *Organometallics* **2000**, *19*, 947−949. (b) Jaquith, J. B.; Levy, C. J.; Bondar, G. V.; Wang, S.; Collins, S. *Organometallics* **1998**, *17*, 914−925. (c) Jaquith, J. B.; Guan, J.; Wang, S.; Collins, S. *Organometallics* **1995**, *14*, 1079−1081. (d) Odenkirk, B.; Bosnich, B. *J. Chem. Soc., Chem. Commun.* **1995**, 1181−1182. (e) Hollis, T. K.; Robinson, N. P.; Bosnich, B. *Organometallics* **1992**, *11*, 2745−2748. (f) Hollis, T. K.; Robinson, N. P.; Bosnich, B. *J. Am. Chem. Soc.* **1992**, *114*, 5464−5466.
(15) Grossman, R. B.; Davis, W. M.; Buchwald, S. L. *J. Am. Chem. Soc.* **1991**, *113*, 2321−2322.
(16) Luinstra, G. A. *J. Organomet. Chem.* **1996**, *517*, 209−215.

Indene, diisopropylamine, triethylamine, *tert*-butylamine, 1,2-dibromoethane, triflic acid, methyl isobutyrate, ethyl isobutyrate, isobutyric acid, thionyl chloride, *n*-BuLi (1.6 M in hexanes), MeMgBr (3.0 M in diethyl ether), dimethyldichlorosilane, lithium dimethylamide, and tetrachlorozirconium were purchased from Aldrich Chemical Co. and used as received, except for the amines which were degassed, dried over CaH_2 overnight, and then vacuum-distilled before use. Trimethylaluminum (neat) was purchased from Strem Chemical Co. and methyllithium (1.6 M in diethyl ether) from Acros.

Methyl methacrylate (MMA) and *n*-butyl methacrylate (BMA) were purchased from Aldrich Chemical Co.; both monomers were first degassed and dried over CaH_2 overnight, followed by vacuum distillation. Final purification involved titration with neat tri(*n*-octyl)aluminum to a yellow end point[17] followed by distillation under reduced pressure. The purified monomers were stored in a −30 °C freezer inside the glovebox.

Tris(pentafluorophenyl)borane, $B(C_6F_5)_3$, was obtained as a research gift from Boulder Scientific Co. and further purified by recrystallization from hexanes at −35 °C. Tris(pentafluorophenyl)alane, $Al(C_6F_5)_3$, as a 0.5•toluene adduct based on the elemental analysis for the vacuum-dried sample, was prepared from the exchange reaction of $B(C_6F_5)_3$ and $AlMe_3$ in a 1:3 toluene/hexanes solvent mixture in quantitative yield according to a literature procedure,[18] which is the modified synthesis of the alane first disclosed by Biagini et al.[19] *Extra caution should be exercised when handling this material because of its thermal and shock sensitivity.*

Neutral ligands, $(EBI)H_2$ (EBI = $C_2H_4(Ind)_2$)[20] and $(SBI)H_2$ (SBI = $Me_2Si(Ind)_2$),[21] were prepared using modified literature procedures. Jordan's stereoselective amine elimination approach[22] was employed to prepare the following five chiral, racemic complexes: *rac*-(EBI)$ZrCl_2$,[23] *rac*-(EBI)$ZrMe_2$,[23] *rac*-(EBI)$Zr(NMe_2)_2$,[23] *rac*-(SBI)$ZrCl_2$,[21] and *rac*-(SBI)$ZrMe_2$;[21] *rac*-(EBI)$ZrMe_2$ was also prepared by Resconi's improved, two-step synthesis.[24] Chloromethyl complexes, *rac*-(SBI)ZrMeCl and *rac*-(EBI)ZrMeCl, were synthesized using a modified method of Andersen and Bergman.[25] Cationic complexes *rac*-(SBI)$ZrMe^+MeM(C_6F_5)_3^-$ and *rac*-(EBI)$ZrMe^+MeM(C_6F_5)_3^-$ (M = B, Al) were generated according to the literature procedure.[26] To facilitate the future discussion to be made in the Results and Discussion section, some key spectroscopic data for *rac*-(EBI)$ZrMe^+MeM(C_6F_5)_3^-$ are listed here. *rac*-(EBI)$ZrMe^+$Me**B**$(C_6F_5)_3^-$: ^{1}H NMR (C_7D_8, 23 °C): δ −0.48 (s, 3H, Zr-Me), −0.66 (s br, 3H, B-Me). ^{19}F NMR (C_7D_8, 23 °C): δ −133.48 (d, 6F, *o*-F), −159.50 (t, 3F, *p*-F), −164.54 (m, 6F, *m*-F). *rac*-(EBI)$ZrMe^+$Me**Al**$(C_6F_5)_3^-$: ^{1}H NMR (C_7D_8, 23 °C): δ −0.70 (s, 3H, Zr-Me), −1.16 (s br, 3H, Al-Me). ^{19}F NMR (C_7D_8, 23 °C): δ −122.78 (d, 6F, *o*-F), −154.29 (t, 3F, *p*-F), −162.00 (m, 6F, *m*-F).

A modified literature method[27] was used to prepare alkyl (isopropyl and *tert*-butyl) isobutyrates and lithium alkyl (methyl, ethyl, isopropyl, and *tert*-butyl)isobutyrates. These lithium ester enolates were isolated in the solid state and stored in a freezer at −30 °C inside the glovebox.

Synthesis of Precursor Complex *rac*-(EBI)Zr(OTf)$_2$. A literature procedure[14b] for the preparation of the analogous tetrahydroindenyl derivative, *rac*-(EBTHI)$Zr(OTf)_2$, was modified for the synthesis of *rac*-(EBI)$Zr(OTf)_2$. In an argon-filled glovebox, a 200-mL Schlenk flask was equipped with a stir bar and charged with 100 mL toluene and 4.27 g (11.3 mmol) *rac*-(EBI)$ZrMe_2$. The flask was sealed with a rubber septum, removed from the glovebox, and interfaced to a Schlenk line. The resulting yellow solution was cooled to −78 °C, and to this solution was quickly added 2.00 mL (3.39 g, 22.6 mmol) triflic acid via syringe. The solution changed instantly to bright orange, with some deep red, insoluble oil. The septum was replaced with a glass stopper, and the reaction was allowed to gradually warm to room temperature over 1 h. Stirring was maintained for 3 h at this temperature, after which the solvent was removed in vacuo. The flask was taken into the glovebox, and the solid residue was extracted with 3 × 70 mL hot toluene. The extract was filtered through a pad of Celite, and the reddish orange filtrate was concentrated to one-half of its volume. The concentrated filtrate was left inside a freezer at −30 °C overnight, yielding 3.20 g of the product after filtration, washing with 2 × 20 mL hexanes, and drying in vacuo. Concentration of the mother liquor and subsequent crystallization afforded an additional 0.44 g of the pure product.

It was observed that *rac*-(EBI)$Zr(OTf)_2$ has limited solubility in toluene but dissolves readily in methylene chloride. Thus, methylene chloride was used to further wash the bright orange residue left on the Celite pad from the above filtration. Evaporation of this filtrate followed by recrystallization from hot toluene yielded an additional 1.50 g of the product. The total isolated yield is 5.14 g (71%).

Alternatively, *rac*-(EBI)$Zr(OTf)_2$ was also prepared from the reaction of *rac*-(EBI)$Zr(NMe_2)_2$ with triflic acid using the same procedure. Although the yield was similar, this route requires no conversion of *rac*-(EBI)$Zr(NMe_2)_2$, the direct product obtained from Jordan's stereoselective amine-elimination synthesis, to the dimethyl derivative *rac*-(EBI)$ZrMe_2$.

^{1}H NMR (C_6D_6, 23 °C) for *rac*-(EBI)$Zr(OTf)_2$: δ 7.21 (d, J = 9.3 Hz, 2H), 7.05−7.00 (m, 6H), 6.86 (d, J = 3.6 Hz, 2H), 5.75 (d, J = 3.3 Hz, 2H), 3.00−2.80 (m, 4H, CH_2CH_2). ^{13}C NMR (bromobenzene-d_5, 23 °C; referenced to residual NMR solvent peaks at 131.63 (t), 130.06 (t), 126.87 (t), 122.91 (s)): δ 131.38, 129.54, 126.64, 125.93, 125.14, 121.58, 121.22, 117.36, 117.15, 110.63, 29.93. ^{19}F NMR (C_6D_6, 23 °C): δ −77.02.

Synthesis of Precursor Complex *rac*-(EBI)ZrMe(OTf). A literature procedure[16] for the preparation of the analogous bis-Cp derivative, Cp_2-ZrMe(OTf), was employed for the synthesis of *rac*-(EBI)ZrMe(OTf). In an argon-filled glovebox, a glass reactor was equipped with a stir bar and charged with 40 mL toluene and 1.89 g (5.00 mmol) *rac*-(EBI)$ZrMe_2$. To this yellow solution was added 3.23 g (5.00 mmol) *rac*-(EBI)$Zr(OTf)_2$ in one portion with vigorous stirring. The solution initially turned to bright red and then faded to yellow. Stirring was maintained for 21 h at ambient temperature, after which the solution was filtered through a pad of Celite. The filtrate was concentrated under reduced pressure to ∼30 mL, layered with 2 mL hexanes, and cooled to −30 °C inside a freezer. The resulting bright yellow crystalline solid collected after filtration was dried in vacuo to give 3.45 g of the first crop of the product. Subsequent concentration of the filtrate and recrystallization from the toluene:hexanes mixture yielded an additional 0.90 g of the product. The total isolated yield is 4.35 g (85%).

^{1}H NMR (C_6D_6, 23 °C) for *rac*-(EBI)ZrMe(OTf): δ 7.30−6.80 (m, 8H), 6.62 (d, J = 3.3 Hz, 1H), 6.33 (d, J = 3.3 Hz, 1H), 5.94 (d, J = 3.3 Hz, 1H), 5.32 (d, J = 3.3 Hz, 1H), 3.10−2.70 (m, 4H, CH_2CH_2), −0.38 (s, 3H, Zr−CH_3). ^{13}C NMR (C_6D_6, 23 °C): δ 127.53, 127.46, 126.95, 126.37, 126.02, 124.53, 124.27, 123.53, 122.80, 121.74, 120.83, 120.61, 118.57, 118.23, 114.73, 113.84, 108.50, 106.57, 43.60 (Zr-CH_3), 28.54 (CH_2), 27.97(CH_2). ^{19}F NMR (C_6D_6, 23 °C): δ −77.36.

(17) Allen, R. D.; Long, T. E.; McGrath, J. E. *Polym. Bull.* **1986**, *15*, 127−134.
(18) Feng, S.; Roof, G. R.; Chen, E. Y.-X. *Organometallics* **2002**, *21*, 832−839.
(19) (a) Biagini, P.; Lugli, G.; Abis, L.; Andreussi, P. U.S. Pat. 5,602269, 1997. (b) Lee, C. H.; Lee, S. J.; Park, J. W.; Kim, K. H.; Lee, B. Y.; Oh, J. S. *J. Mol. Catal., A: Chem.* **1998**, *132*, 231−239.
(20) (a) Grossman, R. B.; Doyle, R. A.; Buchwald, S. L. *Organometallics* **1991**, *10*, 1501−1505. (b) Collins, S.; Kuntz, B. A.; Taylor, N. J.; Ward, D. G. *J. Organomet. Chem.* **1988**, *342*, 21−29.
(21) Christopher, J. N.; Diamond, G. M.; Jordan, R. F.; Petersen, J. L. *Organometallics* **1996**, *15*, 4038−4044.
(22) Diamond, G. M.; Rodewald, S.; Jordan, R. F. *Organometallics* **1995**, *14*, 5−7.
(23) Diamond, G. M.; Jordan, R. F.; Petersen, J. L. *J. Am. Chem. Soc.* **1996**, *118*, 8024−8033.
(24) Balboni, D.; Camurati, I.; Prini, G.; Resconi, L.; Galli, S.; Mercandelli, P.; Sironi, A. *Inorg. Chem.* **2001**, *40*, 6588−6597.
(25) Sweeney, Z. K.; Salsman, J. L.; Andersen, R. A.; Bergman, R. G. *Angew. Chem., Int. Ed.* **2000**, *39*, 2339−2343.
(26) Chen, E. Y.-X.; Kruper, W. J.; Roof, G.; Wilson, D. R. *J. Am. Chem. Soc.* **2001**, *123*, 745−746.
(27) Kim, Y.-J.; Bernstein, M. P.; Galiano Roth, A. S.; Romesberg, F. E.; Williard, P. G.; Fuller, D. J.; Harrison, A. T.; Collum, D. B. *J. Org. Chem.* **1991**, *56*, 4435−4439.

Synthesis of *rac*-(EBI)ZrMe[OC(O^{i}Pr)═CMe$_2$] (1). In an argon-filled glovebox, a 50-mL glass reactor was equipped with a magnetic stir bar, charged with 25 mL toluene, and cooled to −30 °C. To this prechilled reactor, with vigorous stirring, was added 1.02 g (2.00 mmol) *rac*-(EBI)ZrMe(OTf) followed by addition of 0.27 g (2.00 mmol) lithium isopropylisobutyrate. The resulting suspension was stirred for 1 day at ambient temperature, after which it was filtered through a pad of Celite. The solvent of the filtrate was removed in vacuo, yielding 0.87 g (89%) of **1** as a yellow powder. The analytically pure sample was obtained by recrystallization from toluene layered with hexanes at −30 °C inside a freezer of the glovebox. Recrystallization can also be carried out using hexanes at −30 °C.

^{1}H NMR (C_6D_6, 23 °C) for **1**: δ 7.38−6.88 (m, 8H), 6.36 (d, J = 3.3 Hz, 1H), 6.10 (dd, 2H), 5.58 (d, J = 3.3 Hz, 1H), 3.70 (sept, J = 6.3 Hz, 1H, C*H*Me$_2$), 3.20−2.80 (m, 4H, CH_2CH_2), 1.79 (s, 3H, ═C*Me*$_2$), 1.41 (s, 3H, ═C*Me*$_2$), 1.12 (d, J = 6.3 Hz, 3H, −CH*Me*$_2$), 1.08 (d, J = 6.0 Hz, 3H, −CH*Me*$_2$), −0.57 (s, 3H, Zr−CH_3). ^{13}C NMR (C_6D_6, 23 °C): δ 153.88 (O*C*(O^{i}Pr)═), 128.24, 127.57, 127.45, 126.45, 125.01, 124.96, 124.78, 124.41, 124.18, 123.12, 122.42, 120.87, 119.02,115.69, 114.19, 111.91, 105.47, 103.37, 84.59 (═*C*Me$_2$), 67.89 (O*C*HMe$_2$), 31.25 (Zr-*C*H$_3$), 28.71 (CH_2CH_2), 27.76 (CH_2CH_2), 22.55 (OCH*Me*$_2$), 22.47 (OCH*Me*$_2$), 18.12 (═C*Me*$_2$), 17.76 (═C*Me*$_2$). Anal. calcd for $C_{28}H_{32}O_2Zr$: C, 68.39; H, 6.56. Found: C, 68.59; H, 6.77.

Synthesis of *rac*-(EBI)Zr[OC(O^{i}Pr)═CMe$_2$]$_2$ (2). In an argon-filled glovebox, a 50-mL glass reactor was equipped with a magnetic stir bar, charged with 25 mL toluene, and cooled to −30 °C. To this prechilled reactor, with vigorous stirring, was added 0.65 g (1.00 mmol) *rac*-(EBI)Zr(OTf)$_2$ followed by addition of 0.27 g (2.00 mmol) lithium isopropylisobutyrate. The resulting suspension was stirred for 36 h at ambient temperature, after which it was filtered through a pad of Celite. The solvent of the filtrate was removed in vacuo, yielding 0.30 g (50%) of **2** as a yellow powder. The ^{1}H NMR spectrum of this crude material revealed the lithium enolate as the only minor impurity. Crystallization from toluene layered with hexanes at −30 °C was only marginally effective at removing this impurity; however, further recrystallization from a 1:10 toluene/hexanes solvent mixture afforded the analytically pure product. Single crystals suitable for X-ray diffraction studies were grown from hexanes at −30 °C inside a freezer of the glovebox.

^{1}H NMR (C_6D_6, 23 °C) for **2**: δ 7.41 (d, J = 8.4 Hz, 2H), 7.31 (d, J = 8.4 Hz, 2H), 6.91(m, 4H), 6.51(d, J = 3.0 Hz, 2H), 6.03 (d, J = 3.3 Hz, 2H), 3.73 (sept, J = 6.3 Hz, 2H, C*H*Me$_2$), 3.50−3.10 (m, 4H, CH_2CH_2), 1.78 (s, 3H, ═C*Me*$_2$), 1.52 (s, 3H, ═C*Me*$_2$), 1.25 (d, J = 6.3 Hz, 3H, −CH*Me*$_2$), 1.10 (d, 6.0 Hz, 3H, −CH*Me*$_2$). ^{13}C NMR (C_6D_6, 23 °C): δ 154.14 (O*C*(O^{i}Pr)═), 132.78, 125.62, 124.78, 124.56, 122.84, 121.18, 121.09, 115.29, 102.29, 86.23 (═*C*Me$_2$), 68.75 (O*C*HMe$_2$), 29.87 (CH_2CH_2), 23.06 (OCH*Me*$_2$), 22.29 (OCH*Me*$_2$), 18.24 (═C*Me*$_2$), 17.97 (═C*Me*$_2$). Anal. calcd for $C_{34}H_{42}O_4Zr$: C, 67.40; H, 6.99. Found: C, 67.09; H, 6.96.

Synthesis of *rac*-(EBI)Zr$^+$(THF)[OC(O^{i}Pr)═CMe$_2$][MeB(C$_6$F$_5$)$_3$]$^-$ (3). In an argon-filled glovebox, a 30-mL glass reactor was charged with 49.2 mg (0.100 mmol) **1**, 51.2 mg (0.100 mmol) B(C$_6$F$_5$)$_3$, and 10 mL of THF. The resulting orange solution mixture was stirred for 12 h at ambient temperature to produce an orange-red solution. The solvent was removed in vacuo affording a sticky red residue; this residue was then washed with 2 mL hexanes and dried under vacuum for 2 h, producing 0.101 g (93% yield) of the title compound as an orange-red powder.

^{1}H NMR (CD_2Cl_2, 23 °C) for **3**: δ 8.07 (d, J = 8.4 Hz, 1H), 7.94 (d, J = 8.4 Hz, 1H), 7.50−7.26 (m, 6H), 6.65 (d, J = 3.3 Hz, 1H), 6.31 (s, 2H), 6.19 (d, J = 3.3 Hz, 1H), 4.10 (m, 2H, CH_2CH$_2$), 3.92 (m, 2H, CH$_2$CH_2), 3.73 (m, 3H, C*H*Me$_2$, overlapping with α-CH_2, THF), 3.46 (m, 2H, α-CH_2, THF), 2.03 (m, 1H, β-CH_2, THF), 1.83 (m, 3H, β-CH_2, THF), 1.47 (s, 3H, ═C*Me*$_2$), 1.39 (s, 3H, ═C*Me*$_2$), 1.21 (d, J = 6.3 Hz, 3H, −CH*Me*$_2$), 1.06 (d, J = 6.0 Hz, 3H, −CH*Me*$_2$), 0.48 (s, br, 3H, B−CH_3). ^{19}F NMR (CD_2Cl_2, 23 °C): δ −131.53 (d, $^3J_{F-F}$ = 19.5 Hz, 6F, *o*-F), −163.63 (t, $^3J_{F-F}$ = 21.4 Hz, 3F, *p*-F), −166.22 (m, 6F, *m*-F). ^{13}C NMR (CD_2Cl_2, 23 °C): δ 154.07 (O*C*(O^{i}Pr)═), 133.59, 133.02, 128,51, 128.37, 128.17, 127.72, 126.80, 126.72, 124.81, 124.20, 123.80, 123.09, 121.83, 121.10, 118.51, 117.30, 105.36, 104.44 (carbons for the C_6F_5 groups omitted because of C−F coupling), 90.85 (═*C*Me$_2$), 78.67 (α-*C*H$_2$, THF), 67.69 (O*C*HMe$_2$), 30.75 (β-*C*H$_2$, THF), 26.60 (CH_2CH_2), 26.05 (CH_2CH_2), 22.57 (OCH*Me*$_2$), 21.78 (OCH*Me*$_2$), 18.44 (═C*Me*$_2$), 17.31 (═C*Me*$_2$), 10.05 (B-*C*H$_3$). Anal. calcd for $C_{50}H_{40}O_3BF_{15}Zr$: C, 55.82; H, 3.75. Found: C, 55.55; H, 3.93.

Synthesis of *rac*-(EBI)Zr$^+$(Me)OC(O^{i}Pr)OAl(C$_6$F$_5$)$_3^-$ (4). In an argon-filled glovebox, a 30-mL glass reactor was charged with 49.2 mg (0.100 mmol) **1**, 57.4 mg (0.100 mmol) Al(C$_6$F$_5$)$_3$·0.5 toluene, and 10 mL toluene. The resulting orange solution mixture was stirred for 12 h at ambient temperature to produce a yellow-green solution. The solvent was removed in vacuo affording an oily residue; this residue was washed quickly with 4 mL hexanes and dried under vacuum for 2 h, producing 50 mg of the title compound as a yellow solid. Slow cooling the hexane washing to −30 °C afforded an additional 20 mg of the product as yellow needle crystals; the total isolated yield is 70 mg (72%). Single crystals suitable for X-ray diffraction studies were grown from hexanes at −30 °C inside a freezer of the glovebox.

^{1}H NMR (C_6D_6, 23 °C) for **4**: δ 7.25 (d, J = 9.0 Hz, 1H), 7.13 (m, 1H), 6.99 (t, J = 8.4 Hz, 1H), 6.83−6.67 (m, 5H), 6.21 (d, J = 3.3 Hz, 1H), 6.18 (d, J = 3.3 Hz, 1H), 5.96 (d, J = 3.3 Hz, 1H), 5.24 (d, J = 3.3 Hz, 1H), 3.17−3.11 (m, 1H, CH_2CH_2), 2.82−2.63 (m, 3H, CH_2CH_2), 2.01 (sept, J = 6.6 Hz, 1H, C*H*Me$_2$), 0.61 (d, J = 6.6 Hz, 3H, −CH*Me*$_2$), 0.53 (d, J = 6.6 Hz, 3H, −CH*Me*$_2$), −0.72 (s, 3H, Zr−CH_3). ^{19}F NMR (C_6D_6, 23 °C): δ −122.74 (d, $^3J_{F-F}$ = 19.5 Hz, 6F, *o*-F), −152.98 (t, $^3J_{F-F}$ = 19.2 Hz, 3F, *p*-F), −161.68 (m, 6F, *m*-F). ^{13}C NMR (C_6D_6, 23 °C): δ 190.22 (*C*═O), 129.28, 128.51, 127.20, 126.27, 126.06, 125.95, 125.67, 125.53, 123.68, 123.21, 122.48, 121.09, 120.80, 118.13, 114.64, 113.26, 108.12, 104.53 (carbons for the C_6F_5 groups omitted because of C−F coupling), 39.48 (*C*HMe$_2$), 37.99 (Zr−CH$_3$), 28.16 (CH_2CH_2), 27.72 (CH_2CH_2), 19.24 (CH*Me*$_2$), 18.66 (CH*Me*$_2$). Anal. calcd for $C_{43}H_{26}O_2AlF_{15}Zr$: C, 52.82; H, 2.68. Found: C, 52.77; H, 2.94.

X-ray Crystallographic Analyses of 2 and 4. Single crystals suitable for X-ray diffraction studies were quickly covered with a layer of Paratone-N oil (Exxon, dried and degassed at 120 °C/10^{-6} Torr for 24 h) after decanting the mother liquors in the glovebox. The crystals were then mounted on thin glass fibers and transferred into the cold nitrogen steam of a Siemens SMART CCD diffractometer. The structures were solved by direct methods and refined using the Siemens SHELXTL program library.[28] The structures were refined by full-matrix-weighted least-squares on F^2 for all reflections. All non-hydrogen atoms were refined with anisotropic displacement parameters, whereas hydrogen atoms were included in the structure factor calculations at idealized positions. In **4**, there is a disordered hexane molecule in the lattice. Selected crystal data and structural refinement parameters are collected in Table 1.

Polymerization Procedures and Polymer Characterizations. All polymerizations were performed in 30-mL glass reactors in an argon-filled glovebox in toluene or methylene chloride at ambient temperature. For MMA polymerization with the neutral ester enolate **1**, two different approaches—activated monomer and activated catalyst—were used. In the activated monomer approach, B(C$_6$F$_5$)$_3$ (12.0 mg, 23.4 μmol) and 400 equiv of MMA (1.00 mL, 9.35 mmol) were premixed in 3 mL of toluene or CH_2Cl_2. The polymerization was timed immediately after addition of **1** (11.5 mg, 23.4 μmol) in 2 mL of toluene or CH_2Cl_2. In the activated catalyst approach, B(C$_6$F$_5$)$_3$ and complex **1** were premixed in CH_2Cl_2 and stirred for 5 min, and the polymerization was timed immediately after addition of MMA. After the measured time interval, the flask was removed from the glovebox, and the reaction was quenched by adding 5 mL of 5% HCl-acidified methanol. The quenched

(28) Sheldrick, G. M. *SHELXTL*, version 5; Siemens: Madison, WI, 1996.

Table 1. Crystal Data and Structure Refinements for **2** and **4**·C_6H_{14}

	2	**4**·C_6H_{14}
empirical formula	$C_{34}H_{42}O_4Zr$	$C_{49}H_{40}AlF_{15}O_2Zr$
formula weight	605.90	1064.01
temperature/K	173(2)	173(2)
wavelength/Å	0.71073	0.71073
crystal system	monoclinic	monoclinic
space group	*C*2/*c*	*C*2/*c*
a/Å	21.52(2)	27.806(4)
b/Å	11.188(11)	17.103(2)
c/Å	13.016(12)	20.876(3)
α/deg	90	90
β/deg	98.308(17)	122.463(3)
γ/deg	90	90
volume/Å^3	3101(5)	8376.7(19)
Z	4	8
density (calcd)/ Mg/m^3	1.298	1.687
abs coeff/mm^{-1}	0.389	0.394
F(000)	1272	4304
crystal size/mm^3	0.40 × 0.30 × 0.30	0.38 × 0.25 × 0.10
θ range for data collection/°	1.91−23.38	1.47−21.97
index ranges	$-24 \le h \le 23$, $-12 \le k \le 12$ $-14 \le l \le 14$	$-29 \le h \le 29$, $-18 \le k \le 18$ $-21 \le l \le 21$
reflections collected	9255	23610
independent reflections	2259 [$R_{int} = 0.1084$]	5107 [$R_{int} = 0.0973$]
data /restraints/parameters	2259/0/178	5107/0/580
goodness-of-fit on F^2	1.133	1.014
final *R* indices [$I > 2\sigma(I)$]	$R_1 = 0.0721$ $wR_2 = 0.1659$	$R_1 = 0.0482$ $wR_2 = 0.1112$
R indices (all data)	$R_1 = 0.0857$ $wR_2 = 0.1741$	$R_1 = 0.0848$ $wR_2 = 0.1290$
extinction coefficient	0.0001(4)	0.00197(14)
largest diff. peak and hole/eÅ^{-3}	0.955 and −1.016	0.716 and −0.484

mixture was precipitated into 100 mL of methanol, stirred for 1 h, filtered, and washed with methanol. The polymer collected was dried in a vacuum oven at 50 °C overnight to a constant weight.

For MMA polymerization with the preformed cationic ester enolate **3**, 600 equiv of MMA was added to a solution of **3** (15.6 μmol) in 5 mL of CH_2Cl_2 to start the polymerization. In the BMA polymerization, a $[BMA]_0/[\mathbf{3}]_0$ molar ratio of 390 was used. For MMA polymerization with aluminate **4**, 400 equiv of MMA was added to a solution of **4** (23.4 μmol) in 5 mL of toluene to start the polymerization. The workup procedures were identical to those described above for the MMA polymerization by **1**.

Polymer molecular weights and molecular weight distributions were measured by Gel permeation chromatography (GPC) analyses carried out at 40 °C, at a flow rate of 1.0 mL/min, and with THF as the eluent, on a Waters University 1500 GPC instrument. The instrument was calibrated with 10 PMMA standards, and chromatograms were processed with Waters Empower software. ^{1}H NMR spectra for the analysis of PMMA and PBMA microstructures were recorded in $CDCl_3$ and analyzed according to the literature.[29]

Results and Discussion

Synthesis of *ansa*-Zirconocene Ester Enolates. Despite being viscous oils, simple bis(Cp)-type zirconocene mono- or diester enolate complexes can be readily prepared from the reaction of zirconocene mono- or dichlorides with lithium alkylisobutyrates.[1] Employing the same synthetic methodology for the preparation of chiral *ansa*-zirconocene diester enolate

Scheme 1

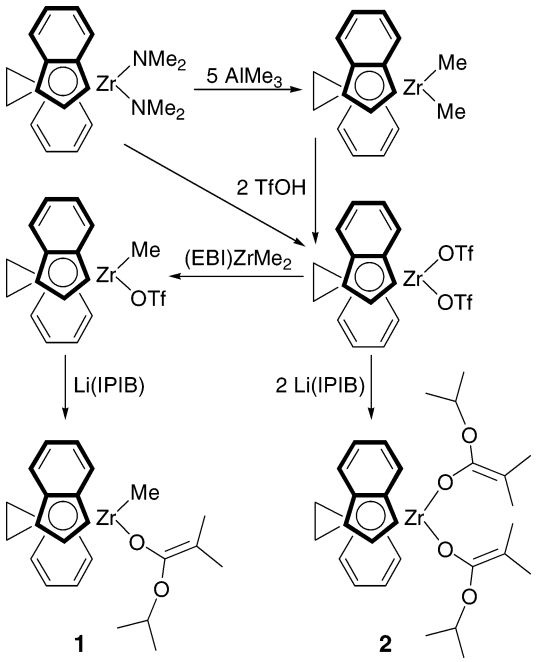

complexes using the reaction of *rac*-(EBI)$ZrCl_2$ with 2 equiv of lithium (or potassium) ester enolates yielded a mixture of products, containing mono- and dienolates, zirconocene alkoxides, and other unidentified species. In efforts to prepare the *ansa*-zirconocene monoester enolates, the reaction between *ansa*-zirconocene monochloro complexes such as *rac*-(EBI)ZrMeCl and *rac*-(SBI)ZrMeCl and 1 equiv of lithium alkyl (Me, Et, ^{i}Pr, ^{t}Bu) ester enolates also produced a mixture of products, often containing zirconocene alkoxide species. In light of these unsuccessful attempts using the chloride precursors and recognizing that the triflate "pseudohalide" anion is a better leaving group than the chloride anion, we sought to investigate the possibility of using *ansa*-zirconocene triflate precursors for this synthesis.

Scheme 1 depicts the reaction schemes leading to *rac*-(EBI)ZrMe[OC(O^{i}Pr)═CMe_2] (**1**) and *rac*-(EBI)Zr[OC(O^{i}Pr)═CMe_2]$_2$ (**2**), through *ansa*-zirconocene triflate intermediates *rac*-(EBI)ZrMe(OTf) and *rac*-(EBI)Zr(OTf)$_2$, respectively. Using the modified literature procedure involving the protonolysis of a dimethyl zirconocene with triflic acid for the preparation of the analogous tetrahydroindenyl derivative,[14b] multigram quantities of *rac*-(EBI)Zr(OTf)$_2$ were isolated in 71% yield from the reaction of *rac*-(EBI)$ZrMe_2$ with TfOH. The dimethyl precursor can be substituted with *rac*-(EBI)Zr(NMe$_2$)$_2$; although a similar yield was achieved, the ability to directly use *rac*-(EBI)Zr(NMe$_2$)$_2$ offers an advantage because of elimination of an additional step for converting the diamide to the dimethyl complex (Scheme 1). On the basis of the literature procedure for the preparation of the $Cp_2ZrMe(OTf)$,[16] *rac*-(EBI)ZrMe(OTf) was isolated in 85% yield from the comproportionation reaction involving *rac*-(EBI)$ZrMe_2$ and *rac*-(EBI)Zr(OTf)$_2$

The reaction of *rac*-(EBI)ZrMe(OTf) with lithium isopropylisobutyrate [Li(IPIB)] in toluene proceeds cleanly to produce the crystalline, monoester enolate **1** in 89% isolated yield. The ^{1}H NMR spectrum (Figure 1) shows C_1-symmetry for **1** in solution, featuring 4 unequivalent protons for the C_5-rings of the bis(indenyl) ligand and two doublets for two diastereotopic

(29) (a) Bovey, F. A.; Mirau, P. A. *NMR of Polymers*; Academic Press: San Diego, CA, 1996. (b) Ferguson, R. C.; Ovenall, D. W. *Macromolecules* **1987**, *20*, 1245−1248. (c) Ferguson, R. C.; Ovenall, D. W. *Polym. Prepr. (Am. Chem. Soc. Div. Polym. Chem.)* **1985**, *26*, 182−183. (d) Subramanian, R.; Allen, R. D.; McGrath, J. E.; Ward, T. C. *Polym. Prepr. (Am. Chem. Soc. Div. Polym. Chem.)* **1985**, *26*, 238−240.

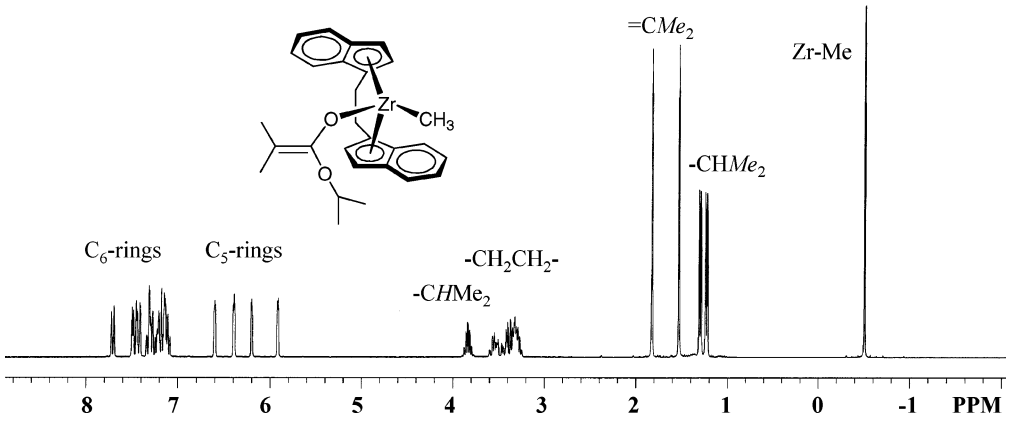

Figure 1. ^{1}H NMR spectrum of **1** in C_6D_5Br.

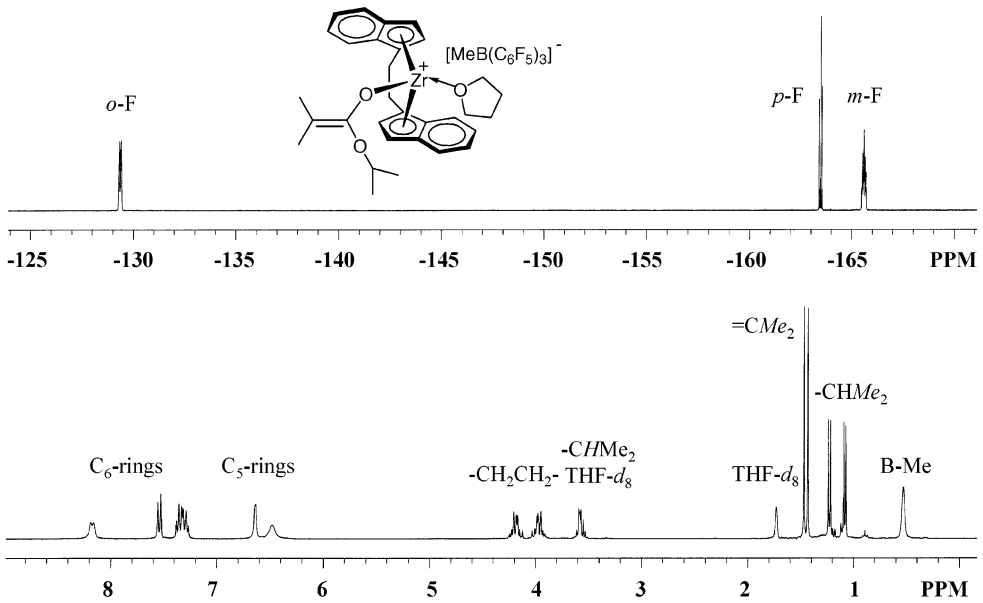

Figure 2. NMR spectra for the in situ generation of **3** by mixing **1** with $B(C_6F_5)_3$ in THF-d_8: ^{1}H NMR (bottom) and ^{19}F NMR (top). For NMR spectral data of the isolated **3**, see Experimental Section.

isopropoxy methyl groups. The analogous reaction of *rac*-(EBI)-$Zr(OTf)_2$ with 2 equiv of Li(IPIB) in toluene was less clean; nevertheless, the pure diester enolate **2** was isolated in 50% yield after repeated recrystallization. The anticipated C_2-symmetry for **2** in solution is evident in the ^{1}H NMR spectrum with only two types of protons for the C_5-rings of the bis(indenyl) ligand. The diester enolate **2** is also a crystalline material, and the molecular structure of **2** was characterized by X-ray diffraction studies (vide infra).

Reaction of *rac*-(EBI)ZrMe[OC(O^{i}Pr)═CMe$_2$] (1) with M-(C_6F_5)$_3$ (M = B, Al). The reaction of zirconocene *ketone* enolates with $B(C_6F_5)_3$ forms direct adducts via borane addition to the enolate carbon center.[9a] To determine if the cationic *ansa*-zirconocene *ester* enolate can be generated or isolated from the monoenolate **1**, the reaction of **1** with $B(C_6F_5)_3$ was investigated in six different solvents. Thus, mixing **1** with $B(C_6F_5)_3$ in toluene, benzene, bromobenzene, or *o*-dichlorobenzene instantaneously formed insoluble, oily precipitates, presumably the cationic complex. The NMR-scale reaction of **1** with $B(C_6F_5)_3$ in CD_2Cl_2 clearly showed the formation of the corresponding cationic zirconocene enolate species; however, the product formed decomposes rapidly, presumably via alkoxide abstraction by Zr. The same reaction, when carried out in THF-d_8, is relatively slower but clean (Figure 2), and the THF-stabilized cationic zirconocene ester enolate (**3**) is stable at room temperature (the solution showed no sign of decomposition for 24 h at room temperature). The ^{1}H NMR spectrum of **3** in the donor solvent THF-d_8 (Figure 2) shows only two broad signals for the C_5-ring protons for time-averaged, C_2-symmetry, suggesting rapid exchange of the free and bound THF ligand.[30] Subsequently, the preparative scale reaction was carried out in THF at room temperature, cleanly producing the cationic zirconocene ester enolate **3** in 93% isolated yield (Scheme 2).

The isolated THF-adduct **3** is also stable in CD_2Cl_2 at room temperature so the full NMR spectroscopic data are reported in CD_2Cl_2 (see Experimental Section). Unlike the ^{1}H NMR spectrum of **3** in THF-d_8 (Figure 2), the spectrum in CD_2Cl_2

(30) This facile ligand exchange between the free and bound THF observed for complex **3** in THF-d_8 appears not to affect the ability of such complexes to perform stereospecific polymerization of methacrylates, as clearly shown by the polymerization results of this work (see polymerization section). The following scenarios may apply: (a) the polymerizations were carried out in toluene or methylene chloride instead of THF; (b) the two lateral coordination sites at Zr are equivalent because of C_2-ligation; and (c) the site switching of the enolate ligand at Zr by exchange of free and bound MMA is slow compared to the rate of propagation.

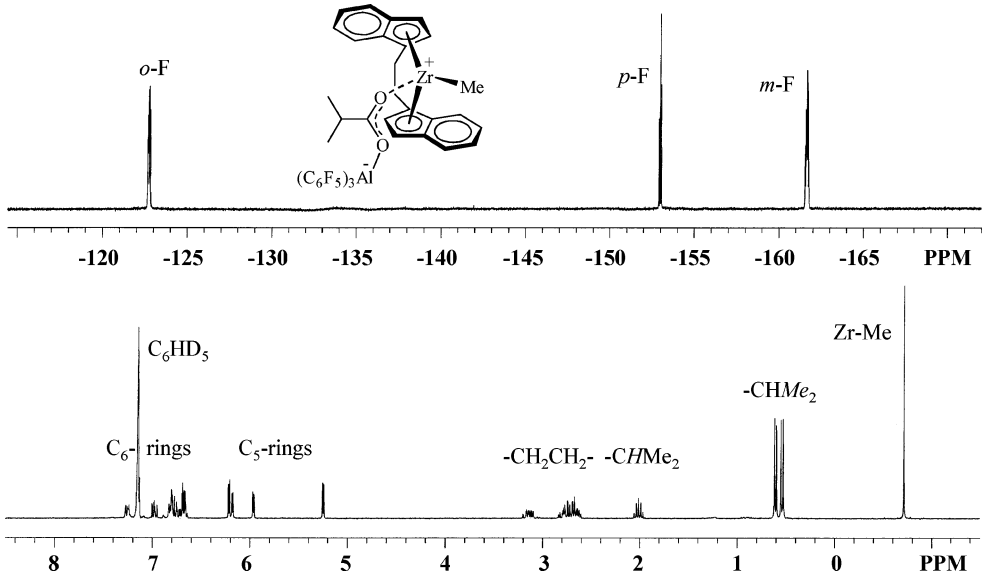

Figure 3. NMR spectra of **4** in C_6D_6: ^{1}H NMR (bottom) and ^{19}F NMR (top).

Scheme 2

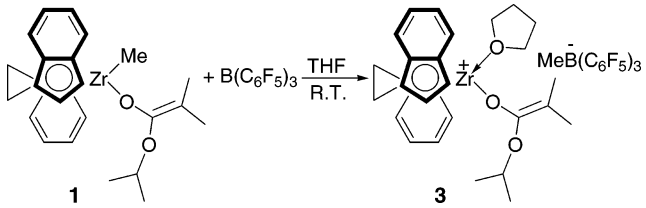

shows C_1-symmetry. Two NMR spectroscopic characteristics of **3** are worth noting. First, in **1** the peak for the methine proton in the $-CH$*Me*$_2$ group appears at lower field than the protons for the ethylene bridge, whereas the chemical shift order in **3** is reversed as a result of the cation formation. Second, the chemical shift for the methyl group in the $[MeB(C_6F_5)_3]^-$ anion is 0.48 ppm in CD_2Cl_2 and 0.53 ppm in THF-d_8, which is nearly the same as that reported in the literature for the free $[MeB(C_6F_5)_3]^-$ anion.[31] The noncoordinating nature of the $[MeB(C_6F_5)_3]^-$ anion in **3** is also established by ^{19}F NMR in which a small chemical shift difference of <3 ppm [$\Delta(m, p\text{-F}) = 2.7$ ppm in **3**] between the *para*- and *meta*-fluorines is diagnostic of the noncoordinating $[MeB(C_6F_5)_3]^-$ anion.[31,32]

Neither THF-d_8 nor CD_2Cl_2 is a suitable solvent for investigating the reactions of **1** with $Al(C_6F_5)_3$, because THF deactivates $Al(C_6F_5)_3$ by forming the stable adduct THF→Al-$(C_6F_5)_3$ and CH_2Cl_2 decomposes $Al(C_6F_5)_3$ via facile chloride abstraction to form $(C_6F_5)_2AlCl$ that exists as a dimer in the solid state.[33] Therefore, this reaction was investigated in benzene or toluene, and fortunately it is homogeneous throughout the reaction. Monitoring the reaction in C_6D_6 by ^{1}H and ^{19}F NMR spectroscopy revealed the rapid formation of initially two major species: the $MeAl(C_6F_5)_3^-$ anion (the pairing cation is presumably *rac*-(EBI)Zr^+[OC(O^{i}Pr)=CMe_2]) and the *rac*-(EBI)$ZrMe^+$ cation (the assumed paring anion Me_2C=C(O^{i}Pr)O$Al(C_6F_5)_3^-$ is, however, not in the final product, vide infra). Significantly, after leaving the solution mixture in the sealed NMR tube for 14 h at room temperature, the $MeAl(C_6F_5)_3^-$ anion, its pairing cation, and other minor species have disappeared and been converted rather cleanly to a single species consisting of the *rac*-(EBI)$ZrMe^+$ cation and a new pairing anion.

The preparative scale reaction afforded spectroscopically the same single species as observed in the NMR-scale reaction in 72% yield. The ^{1}H NMR spectra of this species (Figure 3) features three striking observations: a sharp, distinct *ansa*-bis-(indenyl)Zr^+-Me peak at -0.72 ppm,[34] no peaks assignable for the =C*Me*$_2$ moiety, and substantially high-field shifted peaks for both the methine proton in $-CH$*Me*$_2$ (2.01 ppm) and methyl protons in $-CHMe_2$ (0.61 and 0.53 ppm) as compared to a normal isopropyl isobutyrate ligand in complex **1** (i.e., 3.70 ppm for $-CH$*Me*$_2$, 1.12 and 1.08 ppm for $-CHMe_2$). Additionally, the ^{13}C NMR spectrum shows no peaks in the 85−91 ppm region for the typical =*C*Me$_2$ carbon in complexes **1**−**3**, but exhibits a peak at 190.22 ppm for the C=O group, instead of a peak normally at ∼154 ppm for the (O*C*(O^{i}Pr)=) carbon shown in complexes **1**−**3**. Furthermore, the ^{19}F NMR features a typical, tetracoordinate aluminate.[26] All these lines of evidence point to a conclusion that there is no ester enolate ligand in this complex; rather, all spectroscopic data are consistent with the proposed unique structure **4** consisting of the *rac*-(EBI)$ZrMe^+$ cation paired with the isobutyryl aluminate anion (Scheme 3). The elemental analysis result matched well with the structure **4**, the molecular structure of which has been confirmed by X-ray diffraction studies (vide infra).

Scheme 3 shows the proposed reaction sequence leading to the formation of ion pair **4** through intermediate **5**. In this proposed pathway, the alane-activated isopropylisobutyrate ligand in **5** undergoes intramolecular proton transfer of β−H of the isopropoxy group to the =*C*Me$_2$ carbon followed by elimination of propylene. Monitoring the reaction in the sealed NMR tube indeed showed the initial formation of CH_2=$CHCH_3$ [^{1}H NMR in C_6D_6: 5.71 (m, 1H), 5.04−4.92 (m, 2H), 1.54 (m, 3H)], which was then slowly polymerized to oligomeric propylene by the zirconocenium cation. The initially formed

(31) Klosin, J.; Roof, G. R.; Chen, E. Y.-X.; Abboud, K. A. *Organometallics* **2000**, *19*, 4684−4686.
(32) Horton, A. D.; de With, J.; van der Linder, A. J.; van de Weg, H. *Organometallics* **1996**, *15*, 2672−2674.
(33) Chakraborty, D.; Chen, E. Y.-X. *Inorg. Chem. Commun.* **2002**, *5*, 698−701.
(34) For example, δ (Zr^+-Me) for *rac*-(EBI)$ZrMe^+MeAl(C_6F_5)_3^- = -0.70$ ppm, δ (Zr^+-Me) for *rac*-(SBI)$ZrMe^+MeAl(C_6F_5)_3^- = -0.71$ ppm.

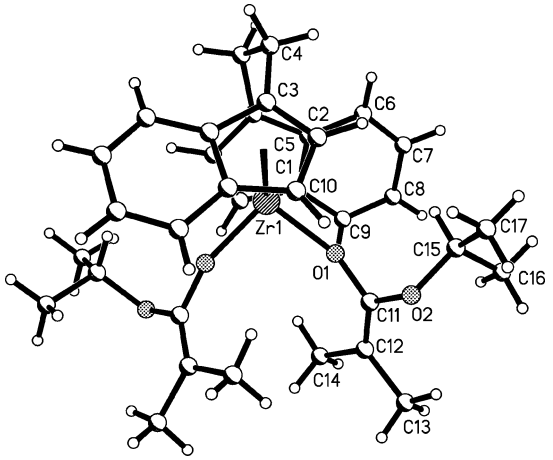

Figure 4. Molecular structure of **2**.

Scheme 3

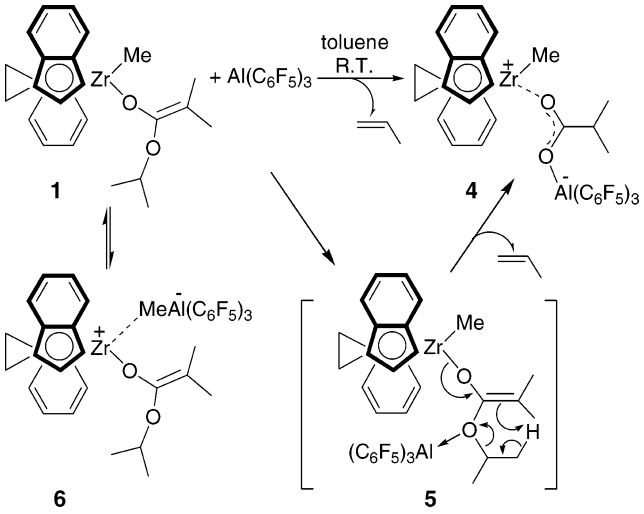

ion-pair **6** disappears gradually during the reaction through a methyl-back transfer from Al to Zr[6b,d] via the **6** ⇌ **1** + Al-$(C_6F_5)_3$ equilibrium (Scheme 3).

Structural Characterizations of *rac*-(EBI)Zr[OC(O^{i}Pr)=CMe$_2$]$_2$ (2) and *rac*-(EBI)Zr$^+$(Me)OC(^{i}Pr)OAl(C$_6$F$_5$)$_3^-$ (4). The molecular structures of **2** and **4** in the solid state are shown in Figures 4 and 5, respectively; important bond distances and angles for these two complexes are tabulated in Tables 2 and 3.

Complex **2** crystallizes in the monoclinic space group *C*2/*c* with C_2-symmetry and the indenyl ligands arranged in the desired *rac*-orientation. Two isopropylisobutyryl ligands are symmetrically bonded to the distorted tetrahedral Zr center with a large Zr−O−C vector angle of 156.6(3)° and a short Zr−O distance of 1.957(4) Å. These metric parameters are similar to those observed for the zirconocene β-keto ester enolate complex $Cp_2ZrMe[OC(Et_2CCOOMe)\text{-}CEt_2]$[12] and the zirconocene ketone enolate complex $Cp_2ZrMe[OC(Me)\text{-}CPh_2]$,[35] suggesting partial double-bond character for the Zr−O bond where the oxygen is partly sp-hybridized because of a p_π–d_π interaction between zirconium and oxygen. The C(11)−C(12) double bond is characterized by a bond distance of 1.305(8) Å and a sum of the angles around C(11) of 360.0° for a trigonal-planar geometry. The two isopropoxy groups are placed into the coordination sphere voids of the *rac*-structure, each facing away from the C_6-rings of the bridged indenyl ligands.

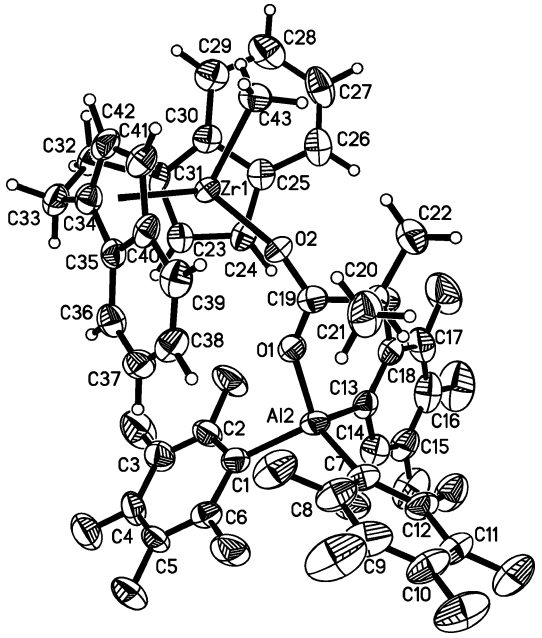

Figure 5. Molecular structure of **4**.

Table 2. Selected Bond Distances (Å) and Angles (deg) for **2**

Zr(1)−O(1)	1.957(4)	Zr(1)−C(1)	2.528(6)
Zr(1)−C(2)	2.493(6)	Zr(1)−C(3)	2.524(6)
Zr(1)−C(5)	2.600(5)	Zr(1)−C(10)	2.627(6)
O(1)−C(11)	1.363(7)	O(2)−C(11)	1.352(7)
O(2)−C(15)	1.432(8)	C(11)−C(12)	1.305(8)
Zr(1)−O(1)−C(11)	156.6(3)	O(1)−Zr(1)−O(#1)	97.4(3)
O(1)−C(11)−O(2)	112.3(5)	O(1)−C(11)−C(12)	123.4(5)
O(2)−C(11)−C(12)	124.3(6)	C(11)−C(12)−C(13)	120.4(7)
C(11)−C(12)−C(14)	123.5(6)	C(13)−C(12)−C(14)	115.9(6)

Table 3. Selected Bond Distances (Å) and Angles (deg) for **4**

Zr(1)−O(2)	2.077(4)	Zr(1)−C(43)	2.243(6)
O(2)−C(19)	1.253(6)	O(1)−C(19)	1.274(6)
O(1)−Al(2)	1.799(4)	Al(2)−C(1)	1.995(6)
Al(2)−C(7)	2.004(6)	Al(2)−C(13)	1.995(6)
Zr(1)−O(2)−C(19)	155.9(4)	C(19)−O(1)−Al(2)	143.6(4)
C(43)−Zr(1)−O(2)	95.39(19)	O(2)−C(19)−O(1)	119.0(5)
O(2)−C(19)−C(20)	119.5(5)	O(11)−C(19)−C(20)	121.5(5)
C(1)−Al(2)−C(7)	113.9(3)	C(1)−Al(2)−C(13)	108.2(2)
C(7)−Al(2)−C(13)	111.8(2)	O(1)−Al(2)−C(1)	104.5(2)
O(1)−Al(2)−C(7)	110.7(2)	O(1)−Al(2)−C(13)	107.3(2)

The molecular structure of the complex **4** features tight ion pairs consisting of the *rac*-(EBI)ZrMe$^+$ cations coordinated through the carboxylate bridge to the isobutyryl aluminate anions. The Zr−O−C vector angle [155.9(4)°] is close to that in the neutral enolate complex **2**, but the C−O−Al vector angle [143.6(4)°] is less obtuse. The Zr−O distance [2.077(4) Å] is 0.12 Å longer than that in complex **2** where the sp-hybridized oxygen and the p_π−d_π interaction between zirconium and oxygen are assumed. The Zr−C(43) distance [2.243(6) Å] compares well with those in the cationic zirconocene methyl complexes.[36] The structure of **4** is best described as a carboxylate bridged mixed metal complex because the C(19)−O(2) [1.253(6) Å] and C(19)−O(1) [1.274(6) Å] bond lengths are

(35) Gambarotta, S.; Strologo, S.; Floriani, C.; Chiesi-Villa, A.; Guastini, C. *Inorg. Chem.* **1985**, *24*, 654−660.

Table 4. MMA and BMA Polymerization Results by Complexes **1**, **3**, and **4**[a]

run no	add. sequence (solvent)	time (min)	yield (%)	10^3M_n[b] (exptl)	PDI[b] (M_w/M_n)	10^3M_n[c] (calcd)	I^*[d] (%)	[*mm*][e] (%)	[*mr*][e] (%)	[*rr*][e] (%)
1	$B(C_6F_5)_3$, MMA, **1** (toluene)	10	>99	48.6	1.03	40.1	83	96.7	2.2	1.1
2	$B(C_6F_5)_3$, MMA, **1** (CH_2Cl_2)	10	>99	46.5	1.03	40.1	86	95.6	3.0	1.4
3	$B(C_6F_5)_3$, **1**, MMA (CH_2Cl_2)	10	97	124	1.10	38.9	31	95.4	3.2	1.4
4	**3**, MMA (CH_2Cl_2)	10	>99	75.5	1.03	60.1	80	95.3	3.2	1.5
5	**3**, BMA (CH_2Cl_2)	120	>99	58.5	1.03	55.5	95	99.1	0.9	0.0
6	**4**, MMA (toluene)	1200	90	51.9	1.93	36.0	69	6.6	34.2	59.2

[a] Carried out in an argon-filled glovebox (<1.0 ppm oxygen and moisture) in toluene or CH_2Cl_2 at ambient temperature. [b] Number-average molecular weight (M_n) and polydispersity index (PDI) determined by GPC relative to PMMA standards. [c] M_n(calcd) = MW (monomer) × [monomer]$_0$/[Zr]$_0$ × conversion. [d] Initiator efficiency (I^*) = M_n(calcd)/M_n(exptl). [e] Tacticity (methyl triad distribution) determined by ^{1}H NMR spectroscopy.

similar and both short, whereas a sum of the angles around C(19) is 360.0° for sp^2-hybridized C(19).

The geometry at the anionic aluminum center is a distorted tetrahedron with a sum of the C−Al−C angles of 333.9°. The average Al−C(aryl) distance (1.998 Å) compares well with those in other $Al(C_6F_5)_3$ complexes with metallocene alkyl,[26,36a] imidazole,[37] toluene,[38] THF,[39] water,[40] and methanol;[40] as expected, the Al−O distance (1.799(4) Å) is noticeably shorter than those observed in the dative-bond adducts of $Al(C_6F_5)_3$ with THF (1.860(2) Å), water (1.857(3) Å), and methanol (1.858(3) Å).

Polymerization of Methacrylates by *rac*-(EBI)ZrMe[OC(O^{i}Pr)=CMe$_2$] (1), *rac*-(EBI)Zr$^+$(THF)[OC(O^{i}Pr)=CMe$_2$]-[MeB(C$_6$F$_5$)$_3$]$^-$ (3), and *rac*-(EBI)Zr$^+$(Me)OC(^{i}Pr)OAl(C$_6$F$_5$)$_3^-$ (4). Neutral zirconocene methyl enolate **1** by itself is inactive for MMA polymerization; however, the polymerization by premixing $B(C_6F_5)_3$ with MMA in toluene followed by addition of **1** ($[MMA]_0/[B(C_6F_5)_3]_0/[\mathbf{1}]_0$ = 400:1:1) is highly active, producing PMMA in quantitative yield in just 10 min. The PMMA formed has an extremely narrow molecular weight distribution (MWD) of M_w/M_n = 1.03 and is highly isotactic ([*mm*] = 96.7%) (run 1, Table 4). In addition to the narrow MWD, the measured M_n is close to, but lower than, the theoretical value, suggesting living behavior of this initiator system with an initiator efficiency of I^* = 83%. The polymerization is enantiomorphic-site controlled, as evidenced by a methyl triad test that gives 2[*rr*]/[*mr*] = 1.0. The same polymerization, but carried out in CH_2Cl_2, has very similar polymerization characteristics (run 2 vs 1).

A reversal of addition sequence, that is, premixing $B(C_6F_5)_3$ with **1** in CH_2Cl_2 for 5 min followed by addition of MMA to start the polymerization, produces PMMA with nearly identical isotacticity; however, the polymer has a significantly higher molecular weight (and a higher PDI value), reflecting a significant drop in initiator efficiency (I^*) from high 86% to low 31% (run 3 vs 2). This observation is attributed to decomposition (vide supra) of the in situ generated cationic zirconocene ester enolate upon mixing $B(C_6F_5)_3$ with **1** in the absence of donor solvent or monomer.

MMA polymerization directly using the THF-stabilized, isolated cationic ester enolate **3** was also investigated. As can be seen from Table 4, polymerization activity, initiator efficiency, and polymer MWD (Figure 6) and isotacticity (Figure 7) of the polymerization by **3** are nearly identical to those of the polymerization by premixing $B(C_6F_5)_3$ with MMA followed by addition of **1** (run 4 vs runs 1 and 2), although in this polymerization a higher $[MMA]_0/[\text{initiator } \mathbf{3}]_0$ ratio (600 vs 400 in runs 1 and 2) was used for the production of higher molecular weight PMMA. This study indicates the same active propagating species—the model structure **3**—is operative in these polymerizations.

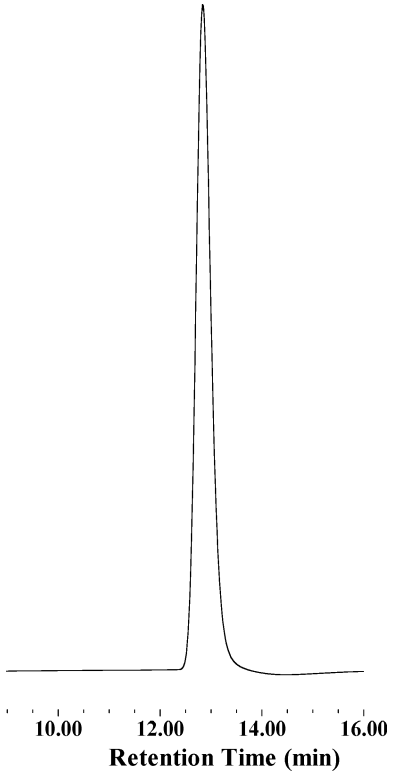

Figure 6. GPC trace of PMMA by **3** (M_n = 75.5 kD, M_w/M_n = 1.03 for run 4, Table 4).

Polymerization of *n*-butyl methacrylate (BMA) by **3** (run 5, Table 4) produces PBMA with nearly perfect isotacticity ([*mm*] > 99%, Figure 8), extremely narrow MWD (M_w/M_n = 1.03), and high initiator efficiency (I^* = 95%), the results of which again suggest living behavior of **3** for polymerization of methacrylates.

The aluminate complex **4**, however, produces syndiotactic PMMA with much broader MWD and lower initiator efficiency (run 6, Table 4). The formation of syndiotactic PMMA by **4** is consistent with our prior observation that C_2-chiral *ansa*-zirconocenes, when activated with $Al(C_6F_5)_3$, produce syndiotactic PMMA predominantly via chain-end control because the

(36) Liu, Z.; Somsook, E.; Landis, C. R. *J. Am. Chem. Soc.* **2001**, *123*, 2915−2916. (b) Chen, E. Y.-X.; Metz, M. V.; Li, L.; Stern, C. L.; Marks, T. J. *J. Am. Chem. Soc.* **1998**, *120*, 6287−6305. (c) Yang, X.; Stern, C. L.; Marks, T. J. *J. Am. Chem. Soc.* **1994**, *116*, 10015−10031.
(37) LaPointe, R. E.; Roof, G. R.; Abboud, K. A.; Klosin, J. *J. Am. Chem. Soc.* **2000**, *122*, 9560−9561.
(38) Hair, G. S.; Cowley, A. H.; Jones, R. A.; McBurnett, B. G.; Voigt, A. *J. Am. Chem. Soc.* **1999**, *121*, 4922−4923.
(39) Belgardt, T.; Storre, J.; Roesky, H. W.; Noltemeyer, M.; Schmidt, H.-G. *Inorg. Chem.* **1995**, *34*, 3821−3822.
(40) Chakraborty, D.; Chen, E. Y.-X. *Organometallics* **2003**, *22*, 207−210.

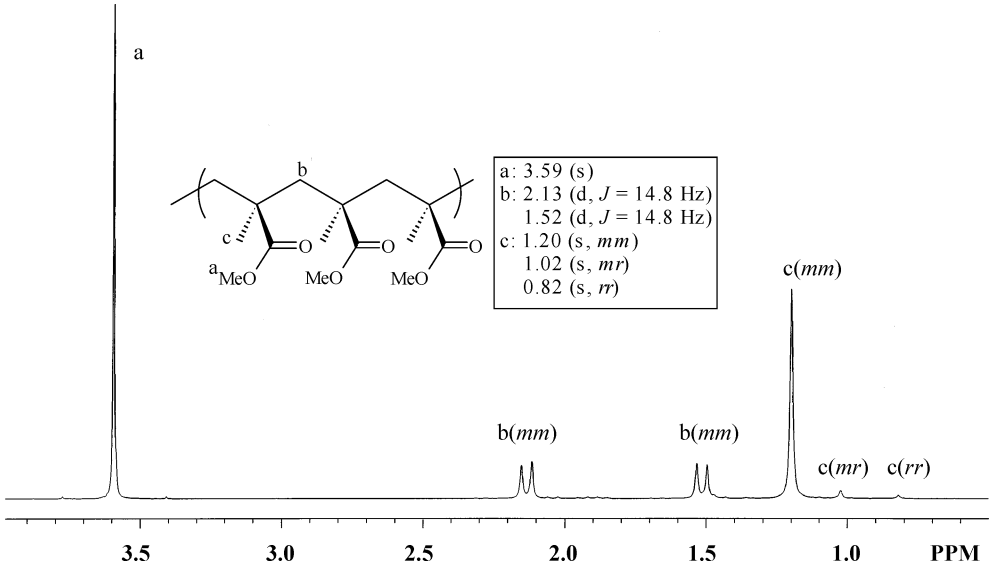

Figure 7. ^{1}H NMR spectrum ($CDCl_3$) and peak assignments of highly isotactic PMMA ([*mm*] = 95.3%, run 4, Table 4) by **3**.

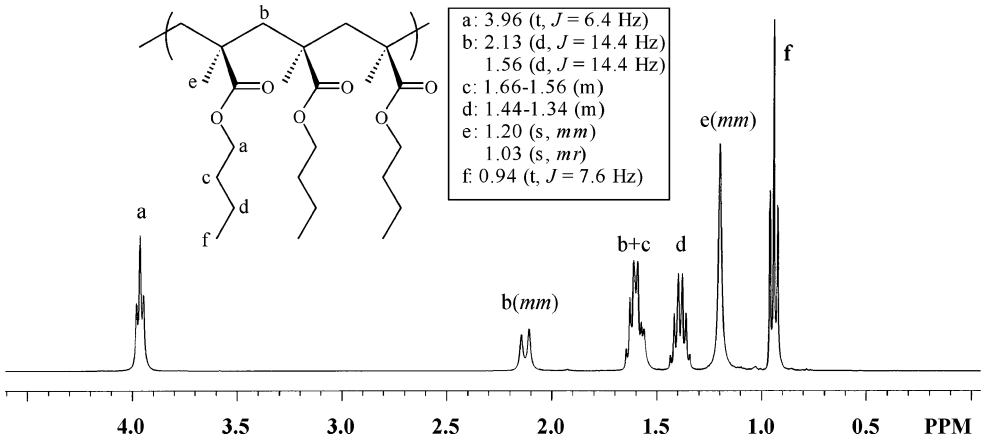

Figure 8. ^{1}H NMR spectrum ($CDCl_3$) and peak assignments of highly isotactic PBMA ([*mm*] = 99.1%, run 5, Table 4) by **3**.

polymer chain propagates at the aluminate anion center, rather than at the cationic zirconocene center.[6d]

In conclusion, we developed an efficient synthesis of *ansa*-zirconocene ester enolates: *rac*-(EBI)ZrMe[OC(O^{i}Pr)═CMe$_2$] (**1**) and *rac*-(EBI)Zr[OC(O^{i}Pr)═CMe$_2$]$_2$ (**2**). To the best of our knowledge, **1** and **2** represent the first examples of chiral *ansa*-zirconocene mono- and diester enolates. The reaction of **1** with $Al(C_6F_5)_3$ in toluene at ambient temperature proceeds through a novel pathway to form the structurally characterized *rac*-(EBI)-Zr^+MeOC(^{i}Pr)OAl$(C_6F_5)_3^-$ (**4**), after elimination of propylene. More significantly, the reaction of **1** with $B(C_6F_5)_3$ in THF cleanly produces the isolable, cationic *ansa*-zirconocene ester enolate *rac*-(EBI)Zr^+(THF)[OC(O^{i}Pr)═CMe$_2$][MeB$(C_6F_5)_3]^-$ (**3**) in quantitative yield. This cationic ester enolate structure is believed to be the active propagating species that bypasses the chain-initiation steps, thereby serving as an excellent structural model (i.e., the proposed structure **A**) for isospecific polymerization MMA mediated by chiral *ansa*-zirconocene complexes.

Preliminary methacrylate polymerization results show that the isolated, cationic ester enolate **3** is both *highly active* and *highly isospecific*, producing polymethacrylates with *extremely narrow MWD*. The polymerization occurs via enantiomorphic-site control and has living characteristics. The polymerization procedure by premixing $B(C_6F_5)_3$ with monomer followed by addition of the neutral **1** has nearly identical polymerization characteristics to those by directly employing cationic **3**; this procedure with neutral **1** presents a convenient, highly efficient, and thus attractive process for polymerization of methacrylates using group 4 metallocene ester enolate complexes.

Acknowledgment. This work was supported by Colorado State University and the donors of the Petroleum Research Fund, administered by the American Chemical Society. We thank Susie M. Miller for determination of the crystal structures and Boulder Scientific Co. for the gift of $B(C_6F_5)_3$. E.Y.C. gratefully acknowledges an Alfred P. Sloan Research Fellowship.

Supporting Information Available: Crystallographic data for **2** and **4** (CIF). This material is available free of charge via the Internet at http://pubs.acs.org.

JA031558K